

Full length article

## Liposomic lubricants suppress acute inflammatory gene regulation in the joint in vivo



Linyi Zhu<sup>a,†,\*</sup>, Weifeng Lin<sup>b,c,†</sup>, Monika Kluzek<sup>b,d,†</sup>, Jadwiga Miotla-Zarebska<sup>a</sup>, Vicky Batchelor<sup>a</sup>, Matthew Gardiner<sup>a</sup>, Chris Chan<sup>a</sup>, Peter Culmer<sup>e</sup>, Anastasios Chanalaris<sup>a</sup>, Ronit Goldberg<sup>b</sup>, Jacob Klein<sup>b,+,\*</sup>, Tonia L. Vincent<sup>a,+</sup>

<sup>a</sup> Kennedy Institute of Rheumatology, Centre for OA Pathogenesis Versus Arthritis, University of Oxford, Roosevelt Drive, Oxford OX3 7FY, UK

<sup>b</sup> Dept. of Molecular Chemistry and Materials Science, Weizmann Institute of Science, Rehovot 7610001, Israel

<sup>c</sup> Key Laboratory of Bio-Inspired Smart Interfacial Science and Technology of Ministry of Education, School of Chemistry, Beihang University, Beijing 100191

<sup>d</sup> IMol, Polish Academy of Sciences; Warsaw, 02-247, Poland

<sup>e</sup> School of Mechanical Engineering, University of Leeds, UK

## ARTICLE INFO

## Keywords:

Biolubrication  
gene regulation  
osteoarthritis  
mouse model  
liposomic lubricants  
articular cartilage

## ABSTRACT

Osteoarthritis (OA) is a widespread, debilitating joint disease associated with articular cartilage degradation. It is driven via mechano-inflammatory pathways, whereby catabolic genes in the cartilage-embedded chondrocytes are presumed up-regulated due to increased shear stress arising from friction at the cartilage surface as joints articulate. The enhanced expression of these cartilage-degrading and inflammatory genes leads to tissue degeneration. However, the nature of the stress, and how the cells within the joint respond to it, are poorly understood. Here we show, in a proof of concept study on a mouse model where surgical joint destabilisation has been carried out to induce OA, that the early up-regulation of the matrix metalloproteinase 3 (*Mmp3*) gene, a member of the matrix-degrading MMP family, and of the interleukin-1 beta (*Il1b*) gene, a key mediator of inflammatory response, are significantly suppressed when lipid-based lubricants are injected into the joints. We attribute this to the reduction in frictional stress on the chondrocytes due to the lubricant at the cartilage surface. At the same time, *Timp1*, a compression but not shear-stress sensitive gene, is unaffected by lubricant. Our results demonstrate that cartilage lubrication modulates catabolic gene regulation in OA, shed strong light on the nature of the chondrocytes' response to shear stress, and have clear implications for novel OA treatments.

**Statement of Significance:** Osteoarthritis (OA) is a widespread, debilitating joint disease associated with degradation of the articular cartilage, the tissue that covers and protects the joint surfaces as they rotate. Such degradation is due to catabolic enzymes expressed by cartilage-embedded chondrocytes (the only cell type in cartilage) in response to mechanical stress. In this proof-of-concept study in a mouse OA model, we show that reduction of cartilage friction by liposome-based lubricants suppresses the production of the catabolic, OA-related genes in chondrocytes. Our findings provide direct evidence in an animal model that catabolic genes are induced in chondrocytes in a mechanosensitive manner, related to the friction at the cartilage surface, and identify putative novel OA treatments through efficient cartilage lubrication.

## 1. Introduction

In healthy joints, the cartilage surfaces are exquisitely lubricated to allow near frictionless motion during articulation [1–3]. Injury to the joint surface or destabilisation of the joint due to ligamentous injury leads to increased shear stress on the superficial cartilage and drives

degradative processes that are associated with the development of osteoarthritis (OA) [4–7], a debilitating disease affecting hundreds of millions worldwide and imposing a large socio-economic burden [8,9]. However, the nature of the stress, and of the cells within the joint that respond to it, are unknown.

Acute injurious mechanical stresses, including those induced in vivo

\* Corresponding authors.

E-mail addresses: [linyi.zhu@kennedy.ox.ac.uk](mailto:linyi.zhu@kennedy.ox.ac.uk) (L. Zhu), [jacob.klein@weizmann.ac.il](mailto:jacob.klein@weizmann.ac.il) (J. Klein).

† These authors contributed equally.

+ Equal contribution.

<https://doi.org/10.1016/j.actbio.2025.04.022>

Received 16 January 2025; Received in revised form 3 April 2025; Accepted 9 April 2025

Available online 10 April 2025

1742-7061/© 2025 The Author(s). Published by Elsevier Inc. on behalf of Acta Materialia Inc. This is an open access article under the CC BY license (<http://creativecommons.org/licenses/by/4.0/>).

by surgically destabilising the knee joint of mice, drive early inflammatory signalling and induce inflammatory genes in chondrocytes, the cells of the articular cartilage [10–13], including matrix degrading enzymes that contribute to the subsequent breakdown of cartilage in OA [14,15]. Previous studies have shown that inflammatory gene regulation in the whole joint occurs rapidly, within 6h of joint destabilisation, but can be abrogated if the joint is completely immobilised (by general anaesthetic or by sciatic neurectomy) immediately after surgery, leading to protection against development of OA [16]. Such immobilisation minimises shear stress by eliminating joint articulation, but allows compressive load to occur on walking. An alternative, which in principle could have a similar effect to joint immobilisation, would be to reduce shear stress by reducing the friction between the cartilage surfaces as they slide past each other. This reduction should correspondingly reduce their catabolic gene regulation [1]. In this study we demonstrate the validity of this concept.

The friction of articular cartilage has been studied for decades [17–19], and recently the use of drug-loaded and other lubricants [20–23] has been considered. While a range of mechanisms has been suggested to account for its remarkably low value [24–28], recent studies have increasingly emphasized the role of hydration lubrication [29–32] by boundary layers (that is, the layers exposed at the surface) exposing highly-hydrated lipid-headgroups at the cartilage surfaces [1, 2]. Indeed it has been explicitly suggested [1] that intra-articular (IA) injection of suitable lipid vesicles would augment cartilage lubrication (i.e. reduce the friction) and thus help to suppress the catabolic gene upregulation underlying OA progression. A number of recent studies [33,34] attempted to examine this idea through IA injection of lubricious nanoparticles, further incorporating anti-inflammatory drugs. In these, however, any regulation in the expression of catabolic enzymes could be attributed to the presence of the incorporated drugs, demonstrating that their efficacy arises from the drugs they delivered [33,34] rather than to lubrication by the nanoparticles. In the present work, in contrast, we determine the effect of lubrication alone (by liposomes) on the chondrocyte gene regulation.

This study aims to explore the impact of lipid-based lubricants on articular cartilage friction and how this impact inhibits the expression of OA-related genes. We examine the lubricating properties of our functionalized liposomes when attached to HA-coated surfaces, as such lipid-HA complexes are a key component of the outer cartilage layer being studied, then measure their retention times in the joint cavity following IA injection, and, separately, their localization on the cartilage surface. In particular, with respect to gene-regulation, we carry out a proof-of-concept study by examining the effect of lubrication on the regulation of a small panel of genes, previously identified by us as highly mechanosensitive and implicated in OA. Among the genes that are known to be regulated within articular chondrocytes upon joint destabilisation we focus on mechano-inflammatory genes with roles in cartilage turnover: matrix metalloproteinase 3 (*Mmp3*) and interleukin 1 beta (*Il1b*), as well as a gene that is mechanically induced in articular cartilage by compressive rather than shear stress, TIMP metalloproteinase inhibitor 1 (*Timp1*). We validate our findings, obtained by quantitative PCR of whole joint and microdissected articular cartilage, using an RNAscope approach which enables visualization of the relevant gene expression in individual cells. This technique, while being more limited in terms of the number of genes that may be studied than by qPCR, provides the most direct evidence to allow us to identify exactly which cells in the cartilage are responding to shear stress and lubricant in vivo.

## 2. Materials and Methods

### 2.1. Animals

Ten-week-old male C57BL/6 mice were purchased either from Jackson Laboratory (retention and cartilage adsorption studies at the Weizmann Institute) or from Charles River (for all other experiments at

the Kennedy Institute of Rheumatology (KIR) in Oxford). Different vendors were dictated by existing contracts within the different universities, though we took care that mice were the same background strain. While modest differences (both genetic and environmental e.g. microbiome) may exist between the sets of mice, we believe it most unlikely that these would have substantially affected the measurements made in this project. Mice at the Weizmann Institute were housed in groups of 1–5 mice per micro-isolator cage in a room with a 12 h light/dark schedule with free access to food and water. Mice at the KIR were kept in an approved animal-care facility and maintained under 12 h light/12 h dark conditions at an ambient temperature of 21°C; housed 4 per cage in standard, individually ventilated cages and were fed with certified mouse diet (RM3; Special Dietary Systems) and water ad libitum. All animal experiments were performed according to the guidelines established by the Weizmann Institute of Science, Rehovot, Israel, and approved by the Institutional Animal Care and Use Committee (IACUC), or following ethical and statutory approval in accordance with local policy at the University of Oxford.

### 2.2. Materials

HSPC (Hydrogenated soybean phosphatidylcholine, Mw 786.11) was purchased from Lipoid GmbH (Germany). DiI Stain (1,10-dioctadecyl-3,3,3,3-tetramethylindocarbocyanine perchlorate C59H97ClN2O4, Mw 933.88) and DiR ((1,1'-Dioctadecyl-3,3,3',3'-Tetramethylindocarbocyanine Iodide, C63H101IN2, Mw 1013.40) and Pierce™ Rapid Gel Clot Endotoxin Assay Kit were provided by ThermoFisher Scientific (Waltham, MA, USA). Cell Proliferation Kit (XTT based) was purchased from Biological Industries (Israel Beit Haemek LTD, Israel). Holey carbon grid (C flat 3/2 200 mesh) was purchased from Electron Microscopy Science (Hatfield, PA, USA). DSPE-pMPC2k (molecular weight of pMPC is ca. 2 kDa) was prepared by two steps according to the reported procedure [35] with minor adjustment, for the subsequent preparation of the HSPC-pMPC liposomes. Poly(allylamine hydrochloride) (PAH, Mw 50000) was purchased from Sigma-Aldrich (Israel). Hyaluronic acid (molecular weight, MW(HA) =  $1.5 \times 10^6$ ) was purchased from CreativePEG (North Carolina, USA). While HA MW may decrease in OA joints, previous work [36] shows little lubrication difference between HA-complexed lipid layers as a function of MW(HA) at physiological pressures. For all IA administration in the in vivo experiments, 33 mM of the HSPC-pMPC liposomes were used; earlier preliminary measurements at much lower doses (11 mM) revealed changes in gene regulation that, unlike the present study, did not reach statistical significance. In future studies we plan to explore also the use of different lubricants.

### 2.3. Preparation of large unilamellar vesicles (LUVs)

Lipids in powder form were dissolved in a chloroform/methanol mixture (2:1, v/v) at a molar ratio of 98% HSPC and 2% DSPE-pMPC (2 kDa). The equivalent mass of each lipid was calculated based on the desired final molar concentration and the molecular weight of each component. Additionally, 0.8% DiI (mol/mol) or 0.1% DiR (mol/mol) was incorporated for cartilage adsorption or retention studies, respectively. For clarity, a typical preparation of 10 mL at a final concentration of 15 mM required 115.2 mg of HSPC, 8.2 mg of DSPE-pMPC (2 kDa), and either 1.1 mg of DiI or 0.2 mg of DiR. The organic solvent was removed by evaporation under a nitrogen stream, followed by vacuum drying for 8 h to ensure complete solvent removal. The resulting lipid film was hydrated with phosphate-buffered saline (PBS; osmolality = 315 mOsm/kg) in a water bath maintained at 70°C to achieve the desired lipid concentration. The suspension was gently vortexed to promote uniform hydration, forming multilamellar vesicles (MLVs). To reduce larger aggregates, the MLV suspension was sonicated for 15 minutes at 70°C. The vesicles were then downsized by extrusion using a Lipex extruder (Northern Lipids Inc.) through polycarbonate membranes with pore sizes of 400 nm and 200 nm. Each extrusion step was

performed 11 times at 65 °C to ensure uniform size distribution. To remove small liposomes and further standardize the sample, the vesicle suspension was centrifuged at 15,000 rpm for 90 minutes. The supernatant was discarded, and the pellet was resuspended in PBS to match the volume of the discarded supernatant. Liposomal samples were tested for endotoxin contamination using the Pierce LAL chromogenic LPS test (Thermo Fisher Scientific, Paisley, UK) following the manufacturer's instructions.

#### 2.4. Evaluation of pMPC-liposomes cytotoxicity

Liposomes cytotoxicity was determined by the production of the yellow formazan product upon cleavage of XTT by mitochondrial dehydrogenases in viable VERO cells (kidney epithelial cell line derived from an African Green Monkey). The cells were seeded onto 96-well plates ( $\sim 4 \times 10^4$  cells/well) in RPMI media (+ 10% FBS + 1% pen/strep). When a confluent state was reached (usually after 24 h), 50  $\mu$ L of pMPC liposomes (at different concentrations up to 1 mM) in PBS solutions were then added. After 24 h and 72 h, the cells were incubated with 50  $\mu$ L of XTT solution composed for 3 h. Absorbance values were later measured with a multiwell-plate reader (Cary 100 Bio, Varian Inc, USA) at a wavelength of 450 nm. Background absorbance was measured at 620 nm and subtracted from the 450 nm measurement. The experiments were repeated at least three times for each liposome concentration. RPMI culture medium was used as a positive control.

The potential toxic effect of the pMPC liposomes tested was expressed as a viability percentage calculated using the following formula:

$$\%Viability = 100 - [(OD_{test} / OD_c) \times 100]$$

Where  $OD_{test}$  was the optical density of those wells treated with the liposome solutions, and  $OD_c$  was the optical density of those wells treated with supplement-free RPMI media. While VERO cells are routinely used as models for cytotoxicity studies [37], in future work we propose to examine the cytotoxicity of the pMPC-functionalized liposomes directly with chondrocyte cells.

#### 2.5. Dynamic light scattering measurements

The size and zeta-potential of the lipid nanoparticles were measured with a ZetaSizer Nano ZS (Malvern Instruments, UK) at 25 °C. Triplicate measurements with a minimum of 10 runs were performed for each sample.

#### 2.6. Cryo-TEM measurements

A Vitrobot Mark IV plunger system was used to prepare the samples for cryo-TEM. Humidity was kept close to 80% for all experiments and the temperature was set at 24 °C. 3.5  $\mu$ L of the sample were placed onto a holey carbon grid (C flat 3/2 200 mesh) which was rendered hydrophilic via glow discharge (Evactron Plasma Cleaning, Evactron, USA). Excess sample was removed by blotting with filter paper and the sample grid was vitrified by rapid plunging into liquid ethane (-180 °C). The grids were kept in liquid nitrogen before being transferred into a Gatan 626 cryo-holder. Cryo-TEM imaging was performed on a FEI Tecnai T12 TEM (120 kV) with a TVIPS F244HD CCD digital camera.

#### 2.7. Cartilage adsorption studies

Liposomes suspension (10  $\mu$ L, 15 mM) was administered intra-articularly (IA) into right knee using BD Micro Fine (30G) syringes under Isoflurane anesthesia. Buprenorphine (10  $\mu$ L, 0.3mg/mL) was intraperitoneal (IP) injected using BD Micro Fine (30G) syringes to relieve pain caused by IA injection. At 6 h, 24 h and 48 h post injections mice were euthanized in their home cages by exposure to carbon dioxide, and joints

were collected.

#### 2.8. Cryo-embedding, sectioning of samples and visualization

Samples were fixed in 4% PFA for 48 h following decalcification for another 48 h in Calci-Clear rapid decalcifying agent (National diagnostics, USA). Samples were then incubated in 30% sucrose solution and embedded in cryo-molds using OCT compound (Tissue-Tek, USA). Seven microns thick coronal section through the middle of the knee joint were prepared using the Leica CM1950 cryotome (Leica Biosystems Newcastle Ltd, UK). Slides were air-dried for 30 minutes following mounting with DAPI-containing mounting media (Fluoromount, BSB-0163 by BioSB USA). Confocal pictures were acquired using a confocal laser scanning fluorescence microscope LSM700 (Zeiss) (Olympus Life Science, Olympus Co., Japan). All images were acquired using a 60X, oil immersion objective, and individual field of view were subsequently stitched together to form the full section. Images were recorded in brightfield mode and in confocal mode using a 561 excitation laser channel. Picture analysis was performed using ImageJ software v1.52i (NIH, USA). For comparative analysis, all parameters during image acquisition were kept constant throughout each experiment.

#### 2.9. Intra-articular retention studies

Mice received IA injections of the pMPC liposomes (10  $\mu$ L, 15 mM) to the right joint space using a BD Micro Fine (30G) syringe under isoflurane anesthesia. The hair around the hind limb surgical sites was removed. Mice were scanned in an IVIS imaging system (PerkinElmer Inc., USA) at different time points. The excitation and emission detectors were set at 760 nm and 780 nm, respectively.

#### 2.10. Surface force balance (SFB) measurements

The SFB (Supplementary Fig. S1) measures directly the normal and shear forces between atomically-smooth mica surfaces (either bare or coated with other species) and is described extensively in previous work, e.g. refs [31,32,38]. The mica surfaces were incubated in PAH solution (0.1 mg/mL) in 0.15 M PBS (0.14 M NaNO<sub>3</sub>) for 5 mins, and then rinsed with 0.15 M PBS (0.14 M NaNO<sub>3</sub>) at 0.10 mg/mL, the solutions were stirred overnight before use. Then, the mica-PAH surface is dipped in a 0.10 mg/mL HA solution. After overnight incubation, the excess HA molecules on the surfaces were rinsed in a beaker containing 200 mL of 0.15 M PBS (0.14 M NaNO<sub>3</sub>). The mica-PAH-HA surfaces were immersed overnight in the HSPC/pMPC2k liposome dispersions (0.3 mM) added to the SFB bath, and the subsequent SFB experiments were carried out in the liposome dispersions. The mean contact pressure  $P$  between the compressed mica surfaces of unperturbed radius of curvature  $R$  under a load  $F_n$  may be estimated as  $P = F_n / (\pi a^2)$  from the Hertzian expression for the contact radius  $a \approx (F_n R / K)^{1/3}$ , where  $K$  is the effective modulus of the mica/glue layer on the crossed cylindrical glass mounts in the SFB. For  $R \approx 0.01$  m and  $K \approx 5.10^9$  N/m<sup>2</sup>, (refs. [31,32]) this yields a pressure of  $P \approx 4$  MPa at the highest values of  $F_n$  (Fig. 1).

#### 2.11. Surgical procedures

Male mice (ages 11-12 weeks) undergoing surgery were anesthetized by inhalation of isoflurane (3% induction and 1.5-2% maintenance) in 1.5-2 L/min oxygen. All mice received a subcutaneous injection of buprenorphine (Vetergesic; Alstoe Animal Health) after surgery. The mice were fully mobile within 4-5 min after the withdrawal of isoflurane. Induction of OA by DMM was performed as previously described [39]. Controls either included naïve (unoperated) animals or sham-operated mice which were anesthetized as for DMM. The numbers used for naïve controls ( $n=4-5$ ) were generally lower as the variance between controls is also low. The right knee was opened using the same

medial parapatellar approach to identify the meniscus without releasing the meniscotibial ligament. The first dose of HSPC-pMPC SUVs (33 mM, 30  $\mu$ L) or PBS was injected into the right knee synovial cavity two-days before surgery (DMM, Sham-operated or Naïve mice) under anaesthetic. The second dose of HSPC-pMPC SUVs or PBS was injected in the joint right after the surgery (DMM or Sham-operated mice) or 6 h before tissue harvesting (naïve mice).

### 2.12. Mouse joint splints

Computer aided design was used to create a splint based on CT scans of a mouse hind limb. The splints were 3D printed in polylactic acid. Following surgery, the splint was slipped over the hind limb to immobilise the knee. The ankle and foot were free to move. Once in position silicone was injected via a side portal in the splint. The liquid silicone filled any gaps between the splint and the limb. A window in the splint over the anterior knee provided access to the wound, which was left uncovered by the silicone. The splint was thin (< 0.75 mm) and light (< 0.8g). In pilot studies, up to seven days, the splints were well-tolerated, activity levels maintained and did not cause skin abrasion. The effect of such a splint resembles that of sciatic neurectomy, which causes paralysis of the hamstring muscles (those that allow flexion of the knee), so the mice have a fixed, fully extended knee joint which can still move through hip flexion. This forces the mouse to swing the leg to the side before it can load weight through it during mobilisation. Essentially, this has exactly the same effect as splinting the joint using the thermoplastic splint as in our study. In other words, compressive load still occurs on walking but surface shear stress is minimised.

### 2.13. RNA extraction and real-time quantitative reverse transcription-polymerase chain reaction (qPCR)

6 h post-surgery, mice were culled by CO<sub>2</sub>. Whole joints were collected and snap-frozen in liquid nitrogen, and then stored at -80 °C. RNA was extracted from the joint using the RNeasy Mini Kit (Qiagen) according to the manufacturer's instructions. Articular cartilage was collected by micro-dissection and kept in RNA later (Invitrogen™, AM7020). Cartilage from four mice was pooled together for RNA isolation to get one data point. Complementary DNA (cDNA) was generated from RNA using a High Capacity cDNA kit (Applied Biosystems) following the manufacturer's instructions. qPCR was run on custom-designed TLDA microfluidic cards ordered from Applied Biosystems. All thermocycling was performed on the ViiA™ 7 system (Applied Biosystems). 50  $\mu$ L of TaqMan Universal PCR Master Mix (Applied Biosystems) were mixed with 50  $\mu$ L cDNA template in nuclease-free water and added to each TLDA loading port. The TLDA card was then centrifuged and sealed. Ct values were obtained after manually choosing the Ct threshold. Expression of the respective genes was normalized to that of 18s as an internal control, using the 2<sup>- $\Delta\Delta$ Ct</sup> method.

### 2.14. In Situ Hybridization and Safo-O staining

Freshly collected whole joints were fixed in 4% (in PBS) ice-cold paraformaldehyde (PFA) for 24 h at 4°C. After washed in ice-cold PBS three times, the joints were applied with increasing sucrose gradient at 4°C: 10%, 20% and 30% sucrose in PBS for 24 h each gradient. Then joints were quickly frozen in Super Cryo Embedding Medium (Section lab, Japan) over dry ice and stored at -80 °C until sectioning on a cryostat. 8  $\mu$ m thickness of coronal section through the middle of the knee joint were collected with Kawamoto's tape (Cryofilm type 3C

(16UF), 2 or 2.5 cm). Kawamoto's tape with a section was then fixed on polysine slide (Fisher brand Superfrost Plus, Fisher Scientific) using Tough-Spots tap (Sigma-aldrich). The slides were air-dried inside the cryotome at -20°C and then kept at -80°C to preserve high RNA integrity.

Prior to hybridization, sections were rinsed with PBS and baked at 60°C for 30 minutes and then dehydrated in increasing concentrations of ethanol (50%, 70%, 95%, 100%, 100%). Sections were incubated with probes for 2 h (*Mmp3*, ACD Cat #. 480961, *Timp1*, ACD Cat # 316841). RNAscope Multiplex Fluorescent Detection kit v2 (ACD, Cat #: 323100) were used to amplify the probe according to the manufacturer's instructions. Opal™ dye (620 Reagent Pack, Akoya Biosciences, Cat # FP1495001KT, 1/1000 dilution) was used for the fluorescence signals as the manufacturer recommended. Slides were coverslipped using ProLong® Gold Antifade Reagent with DAPI (Cell Signaling) and sealed with nail polish. In view of the rapid processing required to image tissues for these experiments, they were done in two independent batches (N=4 in each, i.e. 16 mice).

Adjacent sections were stained with haematoxylin, fast green and safranin O according to a modified protocol to help distinguish the chondrocytes from subchondral bone [40].

### 2.15. Imaging

RNAscope signals were acquired at single-cell resolution (frame size: 4096  $\times$  4096 pixels; pixel size: 0.69  $\mu$ m) on a Zeiss Laser Scanning Microscope (LSM) 880 equipped with seven laser lines (405, 453, 488, 514, 561, 594 and 633 nm). Three tiles covered the whole medial tibia cartilage surface were taken for each joint with a magnification of 40  $\times$ . Safo-O staining images were taken on an Olympus BX51 Osteometric fluorescence microscope.

### 2.16. Transcript quantification in Chondrocytes

Imaris Cell Imaging Software (version 9.0) were used to quantify the transcripts per chondrocytes with supervision by two independent blinded scorers. Quantification of the transcripts was performed using segmentation analysis with a minimum threshold diameter of 0.4  $\mu$ m and 4.0  $\mu$ m for RNA signal and DAPI respectively. Segmentation of the articular cartilage and superficial cartilage were manually drawn with reference to consecutive sections stained using Safranin O. Colocalization analysis was performed for RNA positive cells within the segmented regions of interest.

### 2.17. Shear stress on cartilage-embedded chondrocytes

While we expect, on general grounds of stress balance, that the shear stress within the cartilage layer itself is essentially independent of its depth  $z$  and is given throughout by its value

$$\sigma_s(z) = \sigma_s(z)_{z=0} = \mu P \quad (1)$$

where  $P$  is the contact pressure at the cartilage surface ( $z = 0$ ), this is not the case for the shear *strain*. The shear strain  $\epsilon(z)$  at any depth  $z$  within the cartilage is given by the usual relation  $\epsilon(z) = [\sigma_s(z)/K_{\text{cartilage}}(z)]$  where  $K_{\text{cartilage}}(z)$  is the local rigidity- or shear-modulus of the cartilage at that depth.  $\epsilon(z)$  varies with depth because, as is well established, the modulus  $K_{\text{cartilage}}$  is lower near its surface (superficial zone) than it is deeper down [41,42]. Since the typical rigidity modulus of cells  $K_{\text{cell}}$  – including chondrocytes – is far lower than that of articular cartilage (for which  $K_{\text{cartilage}} = O(10^5 - 10^6 \text{ Pa})$  [41,42], with values  $K_{\text{cell}} = O(100 \text{ Pa})$

[43]), and since the volume fraction of chondrocytes in the cartilage is low (1 – 3%), the strain deformation  $\epsilon_{\text{cell}}$  of the chondrocytes will be determined by the local strain  $\epsilon(z)$  in the cartilage, i.e.

$$\epsilon_{\text{cell}} = \epsilon(z) = [\sigma_s(z)_{z=0} / K_{\text{cartilage}}(z)] \quad (2)$$

The corresponding shear stress  $\sigma_{\text{cell}}(z)$  experienced by the chondrocytes is therefore, from eqs (1) and (2), given by

$$\sigma_{\text{cell}}(z) = (K_{\text{cell}} \times \epsilon_{\text{cell}}(z)) = [K_{\text{cell}} \times \sigma_s(z)_{z=0}] / K_{\text{cartilage}}(z) = \mu P [K_{\text{cell}} / K_{\text{cartilage}}(z)] \quad (3)$$

which is eq 1 in the main text. The foregoing analysis is scale-independent so long as there are significant numbers of cells at different depths to enable differentiation of their behaviour as a function of depth. This is the case here as we are clearly able to differentiate the response in cells in the superficial zone (roughly speaking, within 20  $\mu\text{m}$  of the cartilage surface, or the top two layers of chondrocytes), from cells deeper in the cartilage, as indicated in Fig. 5E.

### 2.18. Statistical Analysis

Data for replicate experiments are expressed as the means  $\pm$  SEM. Analysis was performed using Prism 7 software (GraphPad). Student's *t* tests were used to establish statistical significance between two groups. One-way analysis of variance (ANOVA) was used to compare multiple groups. Two-way ANOVA with Bonferroni's post-test was performed for multiple comparisons. *P* values less than 0.05 were considered statistically significant unless otherwise stated. qPCR studies were powered based on previous measured effect sizes and variance in our laboratory. For RNA Scope, an assumption was made that this would be similar to qPCR. No a priori data analysis plan was published for this study.

## 3. Results

Experiments were carried out in two laboratories (the Kennedy Institute, University of Oxford, and the Weizmann Institute, Rehovot) and care was taken to use the same murine samples (10 –11 weeks-old male C57BL/6 mice) and the same poly(2-methacryloyloxyethyl phosphorylcholine) (pMPC)-functionalized (i.e. pMPCylated-) liposomes throughout in both labs.

### 3.1. Size distribution, morphology and biocompatibility of pMPCylated-liposomes

Large unilamellar vesicles (LUVs) were prepared from hydrogenated soybean phosphatidylcholine (HSPC) lipids functionalized by 2% (mol/mol) pMPC, designated HSPC-pMPC-LUVs ( $^1\text{H}$  NMR see Supplementary Fig. S2). Dynamic light scattering (DLS) measurements (Supplementary Fig. S3) of the liposomes show a uniform, stable size and narrow distribution with a z-average diameter around 170 nm up to 30 days (Supplementary Fig. S3A) and Zeta potential distribution of  $\zeta = -4.2 \pm 0.9$  mV in PBS (Supplementary Fig. S3B), confirmed via Cryo-TEM imaging, where we observe distinct unilamellarity and vesicular morphology (Supplementary Fig. S4B). The size was chosen to maximize retention time in the joint as described earlier [38]. The HSPC-pMPC-LUVs were checked for biocompatibility on VERO cells, showing no significant effect on cell viability for 24 h and 72h (Supplementary Fig. S5).

### 3.2. Lubrication by HSPC-pMPC-LUVs on cartilage mimicking surfaces

As proposed earlier [2,44–49], a key component of the lubricating boundary layers on cartilage comprises lipids (in lamellar or vesicular form) complexed with hyaluronic acid (HA) exposed at the outer cartilage surface. We therefore created HA-exposing surfaces by first coating freshly cleaved, atomically-smooth bare mica with positively charged poly(allylamine hydrochloride) (PAH), followed by incubation in HA solution. After washing away excess HA, HSPC-pMPC-LUVs were added to attach to the surface attached HA layer, and interactions between these HA-liposome-coated surfaces were measured using a surface force balance (SFB) (see Supplementary Fig. S1). The normal force profiles (Fig. 1A) show the onset of repulsion at ca.  $D \approx 300$  nm following addition of the liposomes, consistent with a monolayer of liposomes (diameter ca. 170 nm, Supplementary Fig. S4) attached to the PAH-HA coating on each surface.

The shear force vs. load profiles (Fig. 1B) reveal that friction is strongly reduced once liposomes are complexed with the surface-exposed HA, from  $\mu \approx 0.5$  between PAH-HA coated mica (similar to the value  $\mu \approx 0.3$  measured earlier between HA-coated mica surfaces across water [35]), to  $\mu \approx 0.01 - 0.02$  once the lipids attach to the HA, up to contact pressures of ca. 4 MPa (comparable with physiological pressures in human joints [1]). This  $\mu$  value, while higher than for pMPCylated HSPC-vesicles on bare mica [35] (possibly due to bridging effects [50,51]), is similar to an earlier measurement of friction between mica-attached HA layers complexed with (non-functionalized) DPPC

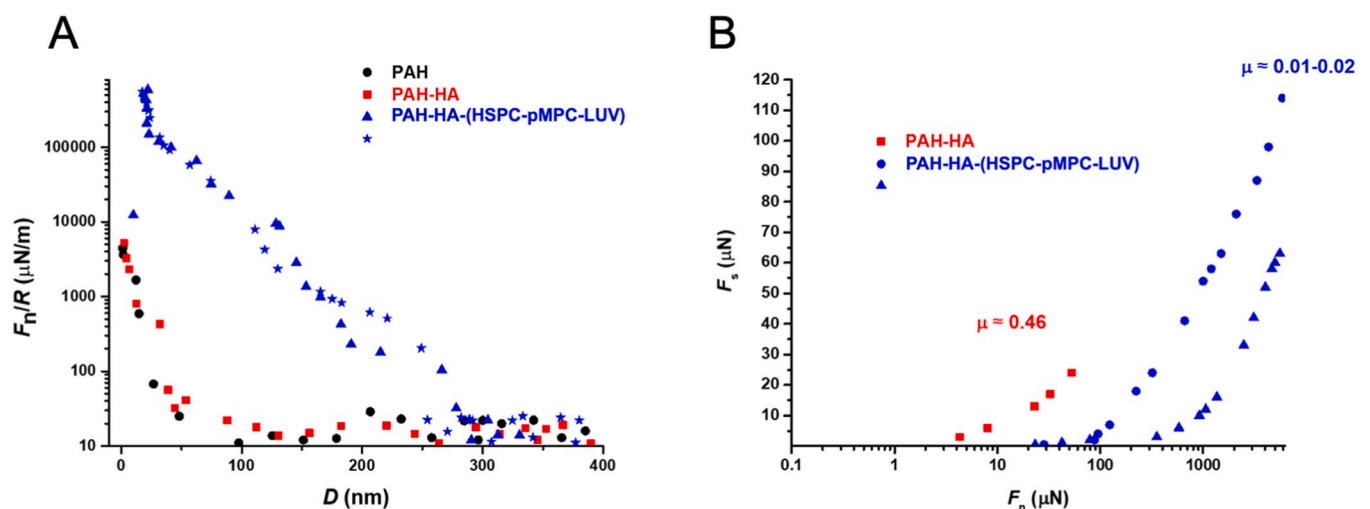
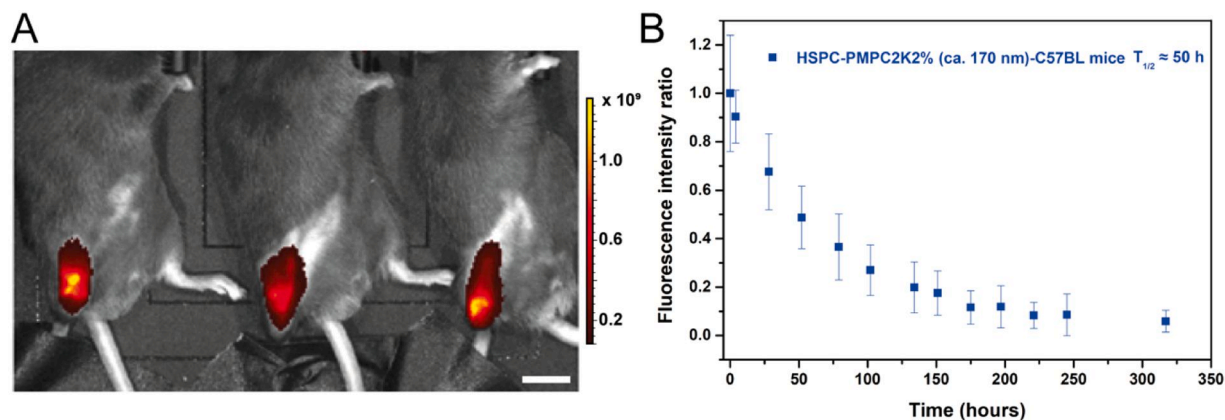


Fig 1. SFB measurements of pMPCylated-liposomes reveal their adsorption on cartilage-mimicking (HA-coated) surfaces across PBS ( $\text{NaNO}_3$ ), and the associated strong friction reduction. (A) forces normalized by radius ( $F_n/R$ ) as a function of surface separation ( $D$ ) (B) friction forces ( $F_s$ ) as a function of applied loads ( $F_n$ ).



**Fig. 2.** Retention kinetics of pMPC-functionalized liposomes following intra-articular injection in naïve mouse joints. (A) IVIS image of 3 repeats of fluorescence intensity for the liposomes injected into knee joints of C57BL/6 mice (at  $t = 153$  h). Scale bar, 10 mm. Radiant efficiency in units of (p/sec/cm<sup>2</sup>/sr)/(mW/cm<sup>2</sup>). (B) Time decay of fluorescence intensity following IA injections, showing  $t_{1/2}$  of  $\sim 50$  h. Mean diameter of the liposome vesicles (determined by DLS, S1A) is ca. 170 nm.

liposomes across salt solutions [47], for which  $\mu \approx 0.01$ . It is also comparable to values reported for friction of cartilage in vivo [3].

### 3.3. Localization and retention of pMPCylated liposomes following injection into joints

HSPC-pMPC-LUVs were fluorescently labelled (DiI) and injected into the joints of naïve C57BL/6 mice (Fig. 2A) to examine their retention and localization. Fig. 2B shows the decay with time of the overall fluorescence intensity of the liposomes in the joint, revealing a retention half-life  $t_{1/2} \approx 50$  hrs, somewhat shorter than the recently reported retention time ( $t_{1/2} \approx 85$  hrs) following IA injection of similarly functionalized HSPC liposomes in a different murine model [52]. Separately, to determine their localization on the cartilage and its time-variation, the liposomes were DiI-labelled and IA injected, following which the mice were sacrificed at different times, and the joints collected, cryo-embedded, sectioned and visualized using confocal microscopy as

shown in Fig. 3.

Fig. 3 shows clearly that the HSPC-pMPC-LUVs attach to the articular surface (Fig. 3A) and, while decreasing substantially by 24 h (Fig. 3B), remain stable at this level on the cartilage at 48 h post-injection (Fig. 3C), indicating, in view of the fact that the cartilage surface is articulating under shear stress over that period, that they are robustly attached. Moreover, as seen in Fig. 3, the liposomes are retained over many days at a lower level in the joint cavity (Fig. 3D) (as also reported earlier in a different study [38]). It is of special interest that both at 6 h (Fig. 3A) where it is clearly seen, but also at 24 and 48 hrs (Fig. 3B, 3C), the fluorescent signal is distributed on the cartilage surface either as a uniform continuous layer (6 h) or quasi-continuously (24, 48 h). In the latter case one would expect the lipids to spread and form a continuous layer on the surfaces when they slide past each other during articulation, as seen when discontinuous lipid micro-reservoirs at a hydrogel surface were slid past a countersurface [53]. Since even a liposome monolayer [52] or a lipid bilayer [53] is sufficient to provide strong boundary

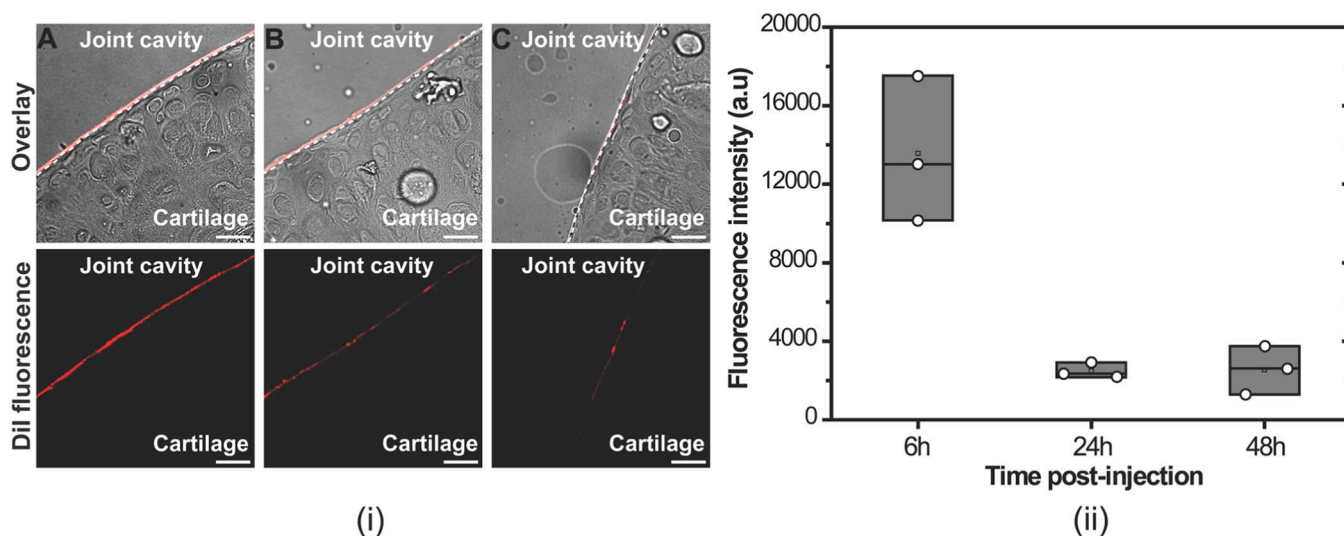


**Fig. 3.** pMPC liposomes injected into naïve mouse joints attach to the cartilage surface. (A–C) Representative confocal microscopy images showing cross-sections of cryo-embedded mouse cartilage at different time points post-injection of pMPC-liposomes containing DiI dye (0.5% mol/mol): (A) 6 h, (B) 24 h, and (C) 48 h. The top row shows overlay images of DiI fluorescence (red) and brightfield, while the bottom row displays DiI fluorescence intensity alone. The white dotted line outlines the interface between the joint cavity and cartilage. Scale bar: 20  $\mu$ m. (D). Retention profile of pMPC-liposomes stained with DiI dye (red). The data represents three independent biological repeats, with each data point an average of at least 10 spots on the cartilage surface for each biological sample. Boxes represent the 25–75 percentiles of the sample distribution (empty squares are mean of the data). Black horizontal lines represent the medians. All fluorescence microscopy data have been normalized to background by subtracting the values obtained for untreated cartilage.

lubrication, this implies that efficient lubrication should readily occur between the articulating cartilage surfaces at least up to 48 hrs post-injection. Confocal images similar to Fig. 3 (Fig. 3A-C) show that the pMPC liposomes attached also to other surfaces in the joint, at a level similar to their attachment to the cartilage surface. We note that the data in Fig. 3 demonstrates the attachment of the liposomes to healthy cartilage; while we believe a similar attachment would occur also on damaged cartilage at a later OA stage, this should be examined directly, as is planned in future work.

### 3.4. Gene expression analysis following joint destabilisation

Two days prior to joint destabilisation, 11-week male C57BL/6 mice received IA injection of either HSPC-pMPC-LUV dispersion or vehicle (PBS). Joints were surgically destabilised by cutting the meniscotibial ligament (also known as destabilisation of the medial meniscus, DMM) [39], and animals were recovered from anaesthesia and allowed to mobilise normally (usually within 15 minutes; we note also that loading of the DMM joints and the unoperated joints was similar [54]). After 6 h the animals were sacrificed and whole joints extracted for RNA analysis of select mechano-sensitive genes (Supplementary Fig. S6A). From previous studies [16] these included genes considered to be shear responsive including *Mmp3*, *Il1b*, and non-shear responsive gene *Timp1* (The RT-PCR experiments were done with a naïve control initially, as the genes selected had already previously been shown to be regulated upon joint destabilisation over sham surgery [16], and the main comparison being made was between DMM and DMM with lubricant). We observed the increase of all three genes following DMM with PBS (Supplementary Fig. S6B). However, when considering the whole joint, we did not see a

difference in the expression level of genes between PBS and HSPC-pMPC-LUV treated groups (Supplementary Fig. S6B). As the whole joint contains multiple tissues, including cartilage, bone, meniscus, synovium as well as non-resident cells, e.g., inflammatory cells that infiltrate the joint in response to surgical injury, it is possible that effects of the DMM on regulation of cells other than the chondrocytes may have diluted the chondrocyte-specific effects of the lubrication. For this reason we decided to examine the articular cartilage separately. Accordingly, we repeated the previous experiment but collected only the cartilage tissue by microdissection for gene expression analysis (Fig. 4A).

DMM surgery upregulated the expression of *Mmp3* (fold-change  $6.36 \pm 2.24$ ), *Il1b* ( $8.63 \pm 3.33$ ) and *Timp1* ( $2.33 \pm 0.52$ ) in the articular cartilage compared with naïve animals (Fig. 4B), but in the presence of the lubricant the increase in shear responsive genes *Mmp3* and *Il1b* was suppressed (down to *Mmp3*,  $4.67 \pm 1.65$ , and *Il1b*  $5.34 \pm 2.26$ ), while the expression level of the non-shear responsive gene, *Timp1*, was not affected ( $2.53 \pm 0.43$ ) (Fig. 4B). In a parallel study the surgically destabilised joint was immobilised immediately after surgery with a thermoplastic splint which allowed weight bearing (joint compression) but prevented knee flexion and hence cartilage surface shear stress (Supplementary Fig. S7A). After 6h, mice were culled and the joints were collected for qRT-PCR as before, showing that, similar to the effect of lubricant addition, such immobilisation suppressed shear associated genes *Mmp3* and *Il1b*, but had no effect on compression-activated gene, *Timp1* (Supplementary Fig. S7B). This result corroborates our finding that intra-articular injection of HSPC-pMPC-LUVs was able to change the biological consequences of joint destabilisation by reducing shear stress on cartilage.

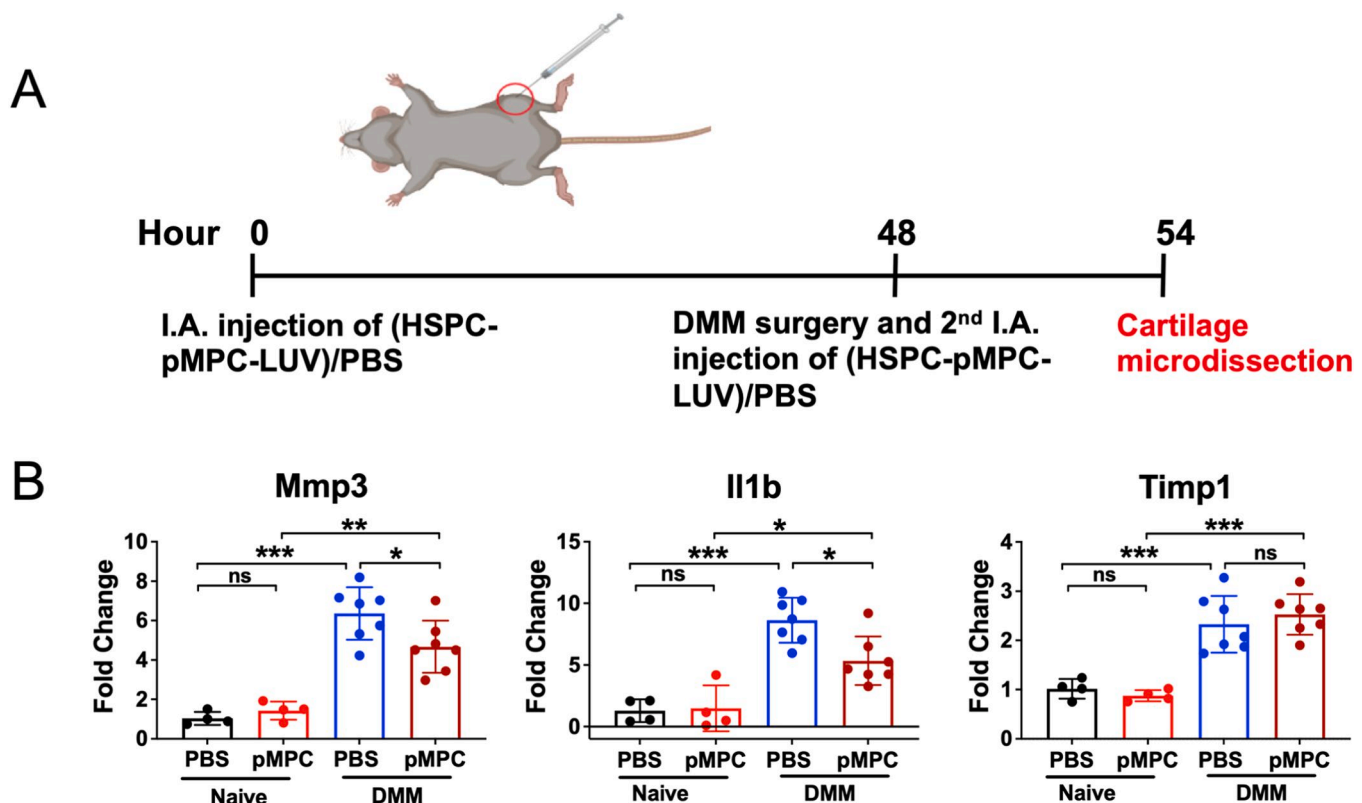


**Fig. 4.** Intra-articular injection of HSPC-pMPC-LUV lubricants suppresses shear-responsive genes in articular cartilage post DMM. (A) Schematic of the time course for the experiments. The right knee joints of male C57BL/6 mice were injected with 30  $\mu$ l of 30 mM HSPC-pMPC-LUVs lubricant or PBS (vehicle) control. 48 h later, at the time of DMM surgery, another IA injection of the lubricant or control was delivered. 6 h post-surgery, cartilage was micro-dissected from knee joints and snap-frozen in RNAlater<sup>TM</sup>. (B) Expression of shear-responsive genes *Mmp3* and *Il1b*, and non-shear responsive gene *Timp1* in the micro-dissected cartilage. Columns labelled 'pMPC' denote injection of the HSPC-pMPC-LUV lubricants. Error bars denote mean  $\pm$  SEM. Results were expressed relative to 18s, and p values were indicated for each gene using two-way ANOVA with Bonferroni's post hoc analysis. \* $p < 0.05$ , \*\* $p < 0.01$ , and \*\*\* $p < 0.001$ . Each data point represents pooled cartilage from 4 mice (88 mice in total, where fewer data points were required for the naïve groups as the variance is smaller).

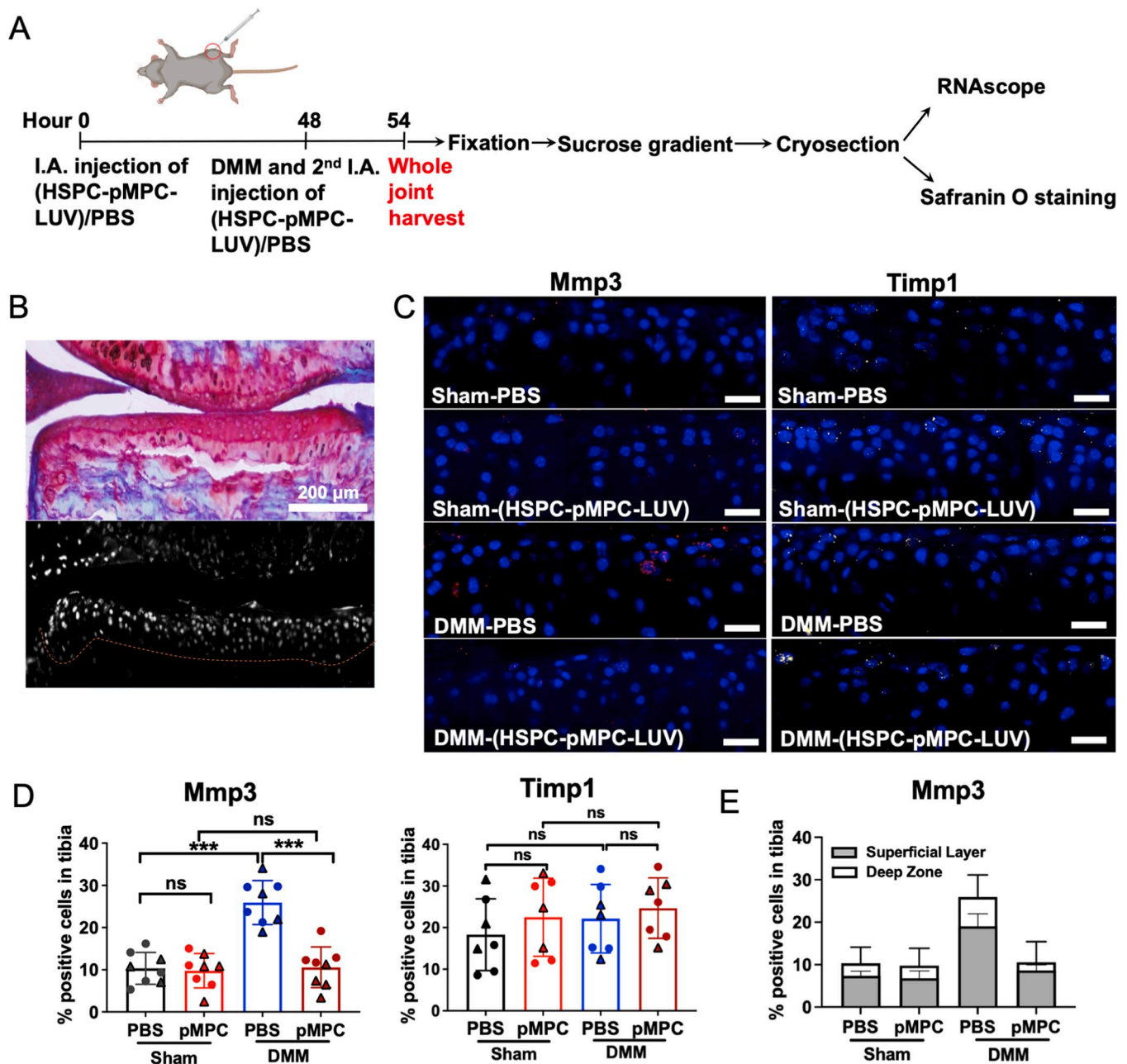


**Fig. 5.** Visualizing the expression of mechano-responsive genes in articular cartilage by RNAscope. (A) Schematic showing the study protocol of the RNAscope and safranin O staining. Mouse whole knee joints were harvested after two doses of intra-articular injection and DMM surgery as before (Fig. 4A) and fixed in 4% ice-cold paraformaldehyde (in PBS) for 24 h. Joints were subjected to an increasing sucrose gradient and sectioned by cryostat (8  $\mu$ m). Adjacent sections were used for RNAscope and safranin O staining. (B) Representative image of safranin O staining (top) and dapi signals (bottom) of adjacent sections from the same knee joint. (C) mRNA transcripts of *Mmp3* (red dots) and *Timp1* (yellow dots) in cartilage from the medial tibia plateau in Sham-PBS, Sham-(HSPC-pMPC-LUV), DMM-PBS and DMM-(HSPC-pMPC-LUV) treated mice. Scale bar, 20  $\mu$ m. (D) Quantification of the *Mmp3*- and *Timp1*-positive cells in tibia cartilage from (C). (E) Distribution of the *Mmp3*-positive cells within the superficial (top two layers of chondrocytes) and deep zones of the tibia cartilage from (C). Columns labelled 'pMPC' denote injection of the HSPC-pMPC-LUV lubricants. p values are indicated for each gene using two-way ANOVA with Bonferroni's post hoc analysis. \*\*p < 0.01, and \*\*\*p < 0.001. n = 8, solid circles and empty triangle represent two independent experiments performed on different days and then combined.

### 3.5. Direct visualization (RNAscope) of gene expression in cartilage-embedded chondrocytes

RNAscope (ACD Bio) is a powerful tool for sensitive detection of mRNA transcripts at high resolution that allows one to visualize the expression of specific genes *in situ*. We repeated the experiment above, save that sham-operated mice (in which the joint was opened but not destabilised) were compared with DMM-operated animals. Each group either had the HSPC-pMPC-LUV or PBS injections according to Fig. 5A.

To overcome the challenges of performing RNAscope on whole, non-decalcified murine joint sections, we adapted a modified protocol (Fig. 5A) [55]. After applying an increased sucrose gradient on the joints, the tissue was sectioned coronally using a cryostat. Adjacent sections from each joint were processed for safranin-O staining and *in situ* hybridization (using the RNAscope Multiplex Fluorescent v2 system). Safranin-O-stained sections were necessary to confirm the integrity of the section after processing and were used to delineate the boundary between cartilage and subchondral bone (Fig. 5B). RNAscope

images were acquired from the medial tibial plateau, the area which degrades first after joint destabilisation and where shear stresses are predicted to be greatest [56]. Images are shown for *Mmp3* and *Timp1* (Fig. 5C) with quantification by counting the percentage of cells showing a positive signal (Fig. 5D). The number of positive cells for *Mmp3* in the DMM-PBS samples ( $25.9 \pm 5.2\%$ ) increased more than two fold compared with the sham-PBS samples ( $10.3 \pm 3.8\%$ ). Injection of HSPC-pMPC-LUVs suppressed the percentage of *Mmp3* positive cells back to the same level as the sham-operated samples ( $10.6 \pm 4.8\%$ ) (Fig. 5D). In contrast, there was no difference in the percentage of the positive cells for the expression of *Timp1* in all four groups, indicating that HSPC-pMPC-LUVs only inhibited the injury-induced shear-responsive genes (Fig. 5D). Importantly, these responses were observed mostly in the superficial chondrocytes, 0–20  $\mu\text{m}$  from the articular surface (2–3 cell layers deep) (Fig. 5E); this is expected because the shear stress on the chondrocytes due to friction at the cartilage surface decays with tissue depth, as later shown.

#### 4. Discussion

The main new finding of this study is that injecting poly(phosphocholinated) liposomic lubricants (HSPC-pMPC-LUVs) into the joints of mice that have been surgically destabilised (DMM), suppresses the early upregulation of shear-stress-sensitive mechano-inflammatory genes including inflammatory cytokines and matrix-degrading enzymes. At the same time, the regulation of a mechanosensitive gene that is non-shear-responsive was unaffected by the injection of the lubricant. These results were corroborated by immobilising the mouse joint using a splint, which reduces joint shear stress by preventing its articulation, but allows compressive load as the mice still bear weight through this limb. Our findings moreover accord with previous work [16], where sciatic neurectomy, which likewise suppresses joint articulation (due to paralysis of the knee flexors), also prevents inflammatory gene regulation whilst preserving compression associated genes. The pMPCylated liposomes used as lubricants, which are known to act as excellent boundary lubricants in model studies [35], are shown to significantly reduce friction also when attached (physically rather than chemically, likely through an entropy-based counterion release mechanism [57]) to an HA-coated substrate used as a simplified in vitro model for the HA-rich articular cartilage surfaces [1,46,49]. These liposomic lubricants are also shown to have in vivo retention time in mouse joints in our study (Fig. 2), which is in line with earlier work [38]. Importantly, they persist as either continuous or quasi-continuous adsorbed layers on the cartilage surface in joints in vivo (Fig. 3), over at least the duration of our study (ca. 2 days).

Together these results point clearly to the following scenario: the IA-injected liposomes form lubricating layers on the articular cartilage in the DMM-operated mice. These result in a reduced friction coefficient  $\mu$  as the joint articulates, where the surface shear stress  $\sigma_s$  is given by  $\sigma_s(z)_{z=0} = \mu P$  at the articular cartilage surface (where  $P$  is the contact pressure between the cartilage surfaces and  $z$  the cartilage depth, where  $z = 0$  denotes the cartilage surface). The effect is to reduce the shear stress throughout the cartilage, and suppress the regulation of shear-stress-sensitive genes, including *Mmp3* and *Il1b*, relative to the unlubricated DMM-operated joint (Figs. 4 and 5). Other joint tissues could be indirectly contributing to the response but this is unlikely, both in view of fact that the effect of the lubricant is to reduce surface shear stress primarily at the cartilage surface, and because of the short response times (within 6 h) which indicate a direct tissue response.

This scenario is further supported when one considers the shear-stress  $\sigma_{s,\text{chondrocyte}}(z)$  experienced by the chondrocytes at different depths  $z$  within the cartilage. Even though it is expected, on general grounds of stress balance, that the shear stress within the cartilage layer itself is essentially independent of the depth  $z$  and is given throughout by its value at the cartilage surface (eq 1, section 2.17), this, counterintuitively, is not the case for the shear stress on the chondrocytes. This is

because, as is well established, the modulus of articular cartilage  $K_{\text{cartilage}}$  is lower near its surface (superficial zone) than it is deeper down [36, 42], while at the same time the typical rigidity modulus of cells  $K_{\text{cell}}$  – including chondrocytes – is far lower than  $K_{\text{cartilage}}$ . Given this it is readily shown that  $\sigma_{s,\text{chondrocyte}}(z)$  is given by (see eq 3 in section 2.17)

$$\sigma_{s,\text{chondrocyte}}(z) = \mu P [K_{\text{cell}}/K_{\text{cartilage}}(z)]$$

Since the rigidity modulus  $K_{\text{cartilage}}(z)$  increases with depth [42], this expression predicts that the shear stress on the chondrocytes decreases with depth. We would therefore expect to see more shear-stress-sensitive genes expressed near the cartilage surface (in the superficial layer) than deeper down. That is exactly what the RNAscope results show, Fig. 5E, where most of the *Mmp3*-positive cells are indeed within the superficial zone. This further supports the concept that it is the lubrication by the HSPC-pMPC-LUVs that is directly responsible for the observed suppression of shear-responsive genes. It is also clear that the articulating cartilage is under normal stresses (i.e.  $P$ ) as well as shear stress. Since it is likely that for most genes there will be a dual contribution to regulation from both normal and shear stresses, this contribution of the normal stress to the regulation may account for why lubricant – which reduces shear but not normal stress – provides significant but not complete inhibition of *Mmp3* and *Il1* in extracted cartilage, as in Fig. 4.

There were a number of limitations in our study. Firstly the RNAscope signals were generally low in our samples compared with published studies using other tissues [55]. This perhaps reflects the chondrocytes' relatively 'quiescent' phenotype or added complexities due to cartilage's highly charged, matrix-rich tissue. This may have contributed to the inability to detect robust regulation of certain genes such as the lack of regulation of *Timp1* on RNAscope after joint destabilisation, even though this was readily observed by RT-PCR when cartilage was microdissected (Fig. 4B). Few of the RNAscope probes have been validated in cartilage previously and additional refinements are likely to be needed in future studies. Secondly, whilst we have shown that there is still detectable lubricant on the cartilage surface at 48h, we do not know whether this remains functional, therefore whether the lubricating activity would persist sufficiently long in between joint injections to modify disease is unknown. Future studies will explore the longer term effects of repeat HSPC-pMPC-LUVs dosing in vivo on development of experimental OA to test this. Our study used two different controls. In the qPCR experiments a naïve (unoperated) control was used, rather than a sham-operated one. Whilst this could be considered a limitation, most of the genes examined had previously been shown by us to be regulated in DMM over the sham control (as demonstrated in Supplementary Fig. S7B), and the primary readout for this experiment was the comparison between DMM-PBS and DMM-(HSPC-pMPC-LUVs). It would also have been instructive to measure shear stress at the cartilage surface in-vivo after joint destabilisation directly by another method. This is challenging to do meaningfully, as measuring torque on the live limb upon forced movement would be dominated by distortion of ligaments and other tissues and swamp the very low cartilage friction, as discussed in refs [1–3]. To some extent, our splinting study (Supplementary Fig. S7) also provides additional support for our gene regulation being driven by surface shear stress. Finally, this study was designed to examine mRNA and did not examine protein levels of the regulated genes.

#### 5. Conclusion

In sum, we demonstrate for the first time the relation between cartilage lubrication in vivo and the regulation of shear-stress-sensitive genes in chondrocytes. This is achieved through IA administration of pMPCylated HSPC liposomes which coat the cartilage surface and act, purely though hydration lubrication at the cartilage surface, with no chemical interactions involved, to reduce the friction and thus the shear stress transmitted to the embedded chondrocytes. Such studies are challenging to deliver in vivo, but offer important insights that are rarely possible using in vitro models. In view of the fact that shear-stress-

sensitive pathways are linked to OA progression [14,15], our results suggest novel treatment modalities, based on IA administration of exogenous liposome-based lubricating agents, for alleviating OA (and its pain-related symptoms) or slowing its progression. Future studies will explore the longer term effects of lubricant dosing in vivo on development of experimental OA.

Supplementary Materials  
Figs. S1 to S7

### Competing interests

The Weizmann Institute has a patent on poly-phosphocholinated-lipid conjugates and liposomes stabilized by such conjugates (US10730976B2), on which WL, RG and JK are co-inventors. RG is a founder of Liposphere, founded 2019; her involvement in this project was prior to this time.

### CRediT authorship contribution statement

**Linyi Zhu:** Writing – review & editing, Writing – original draft, Methodology, Investigation, Formal analysis, Data curation, Conceptualization. **Weifeng Lin:** Writing – review & editing, Writing – original draft, Methodology, Investigation, Data curation, Conceptualization. **Monika Kluzek:** Writing – review & editing, Writing – original draft, Methodology, Investigation, Formal analysis, Data curation, Conceptualization. **Jadwiga Miotla-Zarebska:** Methodology, Investigation. **Vicky Batchelor:** Writing – review & editing, Methodology, Investigation. **Matthew Gardiner:** Writing – review & editing, Writing – original draft, Methodology, Investigation, Formal analysis. **Chris Chan:** Methodology, Formal analysis. **Peter Culmer:** Investigation. **Anastasios Chanalaris:** Investigation. **Ronit Goldberg:** Writing – review & editing, Investigation, Conceptualization. **Jacob Klein:** Writing – review & editing, Writing – original draft, Supervision, Resources, Project administration, Methodology, Investigation, Funding acquisition, Conceptualization. **Tonia L. Vincent:** Writing – review & editing, Supervision, Project administration, Methodology, Formal analysis, Data curation, Conceptualization.

### Declaration of competing interest

The authors declare the following financial interests/personal relationships which may be considered as potential competing interests:

Jacob Klein, Weifeng Lin and Ronit Goldberg has patent #US10730976B2 issued to Weizmann Institute of Science. Ronit Goldberg is a founder of Liposphere Ltd, founded 2019; her involvement in this project was prior to this time. If there are other authors, they declare that they have no known competing financial interests or personal relationships that could have appeared to influence the work reported in this paper.

### Acknowledgements

We thank Sam Safran for useful comments on the ms. We would like to acknowledge Maria Dzamukova and Max Löhning from the Department of Rheumatology and Clinical Immunology, University of Berlin, for sharing the RNAscope protocol. We thank the European Research Council (Advanced Grant CartiLube 743016), the McCutchen Foundation, the Israel Ministry of Science and Technology (Grant 3-15716), and the Israel Science Foundation (Grant 961/24) for financial support. This work was made possible partly through the historic generosity of the Perlman family.

### Supplementary materials

Supplementary material associated with this article can be found, in the online version, at [doi:10.1016/j.actbio.2025.04.022](https://doi.org/10.1016/j.actbio.2025.04.022).

### References

- [1] S. Jahn, J. Seror, J. Klein, Lubrication of articular cartilage, *Annu. Rev. Biomed. Eng.* 18 (1) (2016) 235–258.
- [2] W. Lin, J. Klein, Recent progress in cartilage lubrication, *Adv. Mater.* 33 (18) (2021) 2005513.
- [3] H. Forster, J. Fisher, The influence of loading time and lubricant on the friction of articular cartilage, *Proc. Inst. Mech. Eng. H: J. Eng. Med.* 210 (2) (1996) 109–119.
- [4] K.D. Brandt, P. Dieppe, E.L. Radin, Commentary: is it useful to subset "primary" osteoarthritis? A critique based on evidence regarding the etiopathogenesis of osteoarthritis, *Semin. Arthritis. Rheum.* (2009) 81–95.
- [5] F. Dell'Accio, T. Vincent, Joint surface defects: clinical course and cellular response in spontaneous and experimental lesions, *Eur. Cell. Mater.* 20 (210) (2010) 7.
- [6] M. Englund, A. Guermazi, F.W. Roemer, P. Aliabadi, M. Yang, C.E. Lewis, J. Torner, M.C. Nevitt, B. Sack, D.T. Felson, Meniscal tear in knees without surgery and the development of radiographic osteoarthritis among middle-aged and elderly persons: the Multicenter Osteoarthritis Study, *Arthritis. Rheum.* 60 (3) (2009) 831–839.
- [7] R.B. Frobell, H.P. Roos, E.M. Roos, F.W. Roemer, J. Ranstam, L.S. Lohmander, Treatment for acute anterior cruciate ligament tear: five year outcome of randomised trial, *BMJ* 346 (2013).
- [8] D.J. Hunter, D. Schofield, E. Callander, The individual and socioeconomic impact of osteoarthritis, *Nat. Rev. Rheumatol.* 10 (7) (2014) 437–441.
- [9] S. Safiri, A.-A. Kolahi, E. Smith, C. Hill, D. Bettampadi, M.A. Mansournia, D. Hoy, A. Ashrafi-Asgarabad, M. Sepidarkish, A. Almasi-Hashiani, Global, regional and national burden of osteoarthritis 1990–2017: a systematic analysis of the Global Burden of Disease Study 2017, *Ann. Rheum. Dis.* 79 (6) (2020) 819–828.
- [10] J. Gruber, T.L. Vincent, M. Hermansson, M. Bolton, R. Wait, J. Saklatvala, Induction of interleukin-1 in articular cartilage by explantation and cutting, *Arthritis. Rheum.* 50 (8) (2004) 2539–2546.
- [11] H.M. Ismail, A. Didangelos, T.L. Vincent, J. Saklatvala, Rapid Activation of Transforming Growth Factor  $\beta$ -Activated Kinase 1 in Chondrocytes by Phosphorylation and K63-Linked Polyubiquitination Upon Injury to Animal Articular Cartilage, *Arthritis. Rheum.* 69 (3) (2017) 565–575.
- [12] T.L. Vincent, Mechanoflammation in osteoarthritis pathogenesis, *Semin. Arthritis. Rheum.* 49 (3, Supplement) (2019) S36–S38.
- [13] F.E. Watt, H.M. Ismail, A. Didangelos, M. Peirce, T.L. Vincent, R. Wait, J. Saklatvala, Src and fibroblast growth factor 2 independently regulate signaling and gene expression induced by experimental injury to intact articular cartilage, *Arthritis. Rheum.* 65 (2) (2013) 397–407.
- [14] S.S. Glasson, R. Askew, B. Sheppard, B. Carito, T. Blanchet, H.-L. Ma, C.R. Flannery, D. Peluso, K. Kanki, Z. Yang, Deletion of active ADAMTS5 prevents cartilage degradation in a murine model of osteoarthritis, *Nature* 434 (7033) (2005) 644–648.
- [15] C.B. Little, A. Barai, D. Burkhardt, S. Smith, A. Fosang, Z. Werb, M. Shah, E. Thompson, Matrix metalloproteinase 13-deficient mice are resistant to osteoarthritic cartilage erosion but not chondrocyte hypertrophy or osteophyte development, *Arthritis. Rheum.* 60 (12) (2009) 3723–3733.
- [16] A. Burleigh, A. Chanalaris, M.D. Gardiner, C. Driscoll, O. Boruc, J. Saklatvala, T. L. Vincent, Joint immobilization prevents murine osteoarthritis and reveals the highly mechanosensitive nature of protease expression in vivo, *Arthritis. Rheum.* 64 (7) (2012) 2278–2288.
- [17] D. Dowson, Paper R2: Review of Symposium on Lubrication and Wear in Living and Artificial Human Joints, London, April 1967, in: *Proceedings of the Institution of Mechanical Engineers, Conference Proceedings*, SAGE Publications Sage UK: London, England, 1966, pp. 226–231.
- [18] V. Wright, Lubrication and wear in joints, Sector Publishing Limited, 1969.
- [19] G. Jay, J. Torres, M. Warman, M. Laderer, K. Breuer, The role of lubricin in the mechanical behavior of synovial fluid, *Proc. Natl. Acad. Sci. U S A* 104 (15) (2007) 6194–6199.
- [20] P. Gong, C. Qi, D. Wang, M. Chao, J. Liu, M. Cai, W. Liu, Fluorinated graphene quantum dots with long-term lubrication for visual drug loading and joint inflammation therapy, *Friction* 11 (12) (2023) 2204–2220.
- [21] P. Gong, M. Wang, J. Wang, J. Li, B. Wang, X. Bai, J. Liu, Z. Liu, D. Wang, W. Liu, A biomimetic lubricating nanosystem for synergistic therapy of osteoarthritis, *J. Colloid Interface Sci.* 672 (2024) 589–599.
- [22] C. Li, P. Gong, M. Chao, J. Li, L. Yang, Y. Huang, D. Wang, J. Liu, Z. Liu, A biomimetic lubricating nanosystem with responsive drug release for osteoarthritis synergistic therapy, *Adv. Healthc. Mater.* 12 (12) (2023) 2203245.
- [23] D. Wang, J. Li, C. Niu, Y. Wu, S. Gong, Z. Liu, J. Liu, P. Gong, W. Liu, Biomimetic lubricating COFs with donor-acceptor structure for osteoarthritis therapy, *J. Colloid Sci.* 687 (2025) 85–94.
- [24] B. Hills, Boundary lubrication in vivo, *Proc. Inst. Mech. Eng. H: J. Eng. Med.* 214 (1) (2000) 83–94.
- [25] A. Maroudas, Research Report 2: Hyaluronic Acid Films, in: *Proceedings of the Institution of Mechanical Engineers, Conference Proceedings*, SAGE Publications Sage UK: London, England, 1966, pp. 122–124.
- [26] C. McCutchen, Mechanism of animal joints: sponge-hydrostatic and weeping bearings, *Nature* 184 (4695) (1959) 1284–1285.
- [27] T.A. Schmidt, N.S. Gastelum, Q.T. Nguyen, B.L. Schumacher, R.L. Sah, Boundary lubrication of articular cartilage: role of synovial fluid constituents, *Arthritis. Rheum.* 56 (3) (2007) 882–891.
- [28] D. Dowson, Bio-tribology, *Faraday Discuss.* 156(1) (2012) 9–30.
- [29] W.H. Briscoe, S. Titmuss, F. Tiberg, R.K. Thomas, D.J. McGillivray, J. Klein, Boundary lubrication under water, *Nature* 444 (7116) (2006) 191–194.
- [30] J. Klein, Hydration lubrication, *Friction* 1 (1) (2013) 1–23.

- [31] L. Ma, A. Gaisinskaya-Kipnis, N. Kampf, J. Klein, Origins of hydration lubrication, *Nat. Commun.* 6 (1) (2015) 6060.
- [32] U. Raviv, J. Klein, Fluidity of bound hydration layers, *Science* 297 (5586) (2002) 1540–1543.
- [33] H. Chen, T. Sun, Y. Yan, X. Ji, Y. Sun, X. Zhao, J. Qi, W. Cui, L. Deng, H. Zhang, Cartilage matrix-inspired biomimetic superlubricated nanospheres for treatment of osteoarthritis, *Biomater* 242 (2020) 119931.
- [34] Y. Lei, Y. Wang, J. Shen, Z. Cai, C. Zhao, H. Chen, X. Luo, N. Hu, W. Cui, W. Huang, Injectable hydrogel microspheres with self-renewable hydration layers alleviate osteoarthritis, *Sci. Adv.* 8 (5) (2022) eabl6449.
- [35] W. Lin, N. Kampf, R. Goldberg, M.J. Driver, J. Klein, Poly-phosphocholinated liposomes form stable superlubrication vectors, *Langmuir* 35 (18) (2019) 6048–6054.
- [36] Z. Liu, W. Lin, Y. Fan, N. Kampf, Y. Wang, J. Klein, Effects of hyaluronan molecular weight on the lubrication of cartilage-emulating boundary layers, *Biomacromolecules* 21 (10) (2020) 4345–4354.
- [37] A.L. Perryman, J.S. Patel, R. Russo, E. Singleton, N. Connell, S. Ekins, J. S. Freundlich, Naïve Bayesian Models for Vero Cell Cytotoxicity, *Pharm. Res.* 35 (9) (2018) 170.
- [38] W. Lin, R. Goldberg, J. Klein, Poly-phosphocholination of liposomes leads to highly-extended retention time in mice joints, *J. Mater. Chem. B* 10 (15) (2022) 2820–2827.
- [39] S. Glasson, T. Blanchet, E. Morris, The surgical destabilization of the medial meniscus (DMM) model of osteoarthritis in the 129/SvEv mouse, *Osteoarthritis Cartilage* 15 (9) (2007) 1061–1069.
- [40] T. Kawamoto, K. Kawamoto, Preparation of thin frozen sections from nonfixed and undecalcified hard tissues using Kawamoto's film method, in: *Skeletal development and repair: methods and protocols*, 2014, Springer, 2012, pp. 149–164.
- [41] J.L. Silverberg, A.R. Barrett, M. Das, P.B. Petersen, L.J. Bonassar, I. Cohen, Structure-function relations and rigidity percolation in the shear properties of articular cartilage, *Biophys. J.* 107 (7) (2014) 1721–1730.
- [42] J.L. Silverberg, S. Dillavou, L. Bonassar, I. Cohen, Anatomic variation of depth-dependent mechanical properties in neonatal bovine articular cartilage, *J. Orthop. Res.* 31 (5) (2013) 686–691.
- [43] W.J. Eldridge, S. Ceballos, T. Shah, H.S. Park, Z.A. Steelman, S. Zauscher, A. Wax, Shear modulus measurement by quantitative phase imaging and correlation with atomic force microscopy, *Biophys. J.* 117 (4) (2019) 696–705.
- [44] P. Hilser, A. Suchánková, K. Mendová, K.E. Filipič, M. Daniel, M. Vrbka, A new insight into more effective viscosupplementation based on the synergy of hyaluronic acid and phospholipids for cartilage friction reduction, *Biotribology* 25 (2021) 100166.
- [45] T. Murakami, S. Yarimitsu, K. Nakashima, Y. Sawae, N. Sakai, Influence of synovia constituents on tribological behaviors of articular cartilage, *Friction* 1 (2013) 150–162.
- [46] A. Raj, M. Wang, T. Zander, D.F. Wieland, X. Liu, J. An, V.M. Garamus, R. Willumeit-Römer, M. Fielden, P.M. Claesson, Lubrication synergy: Mixture of hyaluronan and dipalmitoylphosphatidylcholine (DPPC) vesicles, *J. Colloid Interface Sci.* 488 (2017) 225–233.
- [47] J. Seror, L. Zhu, R. Goldberg, A.J. Day, J. Klein, Supramolecular synergy in the boundary lubrication of synovial joints, *Nat. Commun.* 6 (1) (2015) 6497.
- [48] M. Wang, C. Liu, E. Thormann, A. Dedinaite, Hyaluronan and phospholipid association in biolubrication, *Biomacromolecules* 14 (12) (2013) 4198–4206.
- [49] L. Zhu, J. Seror, A.J. Day, N. Kampf, J. Klein, Ultra-low friction between boundary layers of hyaluronan-phosphatidylcholine complexes, *Acta Biomater* 59 (2017) 283–292.
- [50] A. Gaisinskaya-Kipnis, J. Klein, Normal and frictional interactions between liposome-bearing biomacromolecular bilayers, *Biomacromolecules* 17 (8) (2016) 2591–2602.
- [51] W. Lin, Z. Liu, N. Kampf, J. Klein, The role of hyaluronic acid in cartilage boundary lubrication, *Cells* 9 (7) (2020) 1606.
- [52] R. Goldberg, A. Schroeder, G. Silbert, K. Turjeman, Y. Barenholz, J. Klein, Boundary lubricants with exceptionally low friction coefficients based on 2D close-packed phosphatidylcholine liposomes, *Adv. Mater.* 23 (31) (2011) 3517.
- [53] W. Lin, M. Kluzek, N. Iuster, E. Shimoni, N. Kampf, R. Goldberg, J. Klein, Cartilage-inspired, lipid-based boundary-lubricated hydrogels, *Science* 370 (6514) (2020) 335–338.
- [54] I.S. von Loga, V. Batchelor, C. Driscoll, A. Burleigh, S.L.L. Chia, B. Stott, J. Miotla-Zarebska, D. Riley, F. Dell'Accio, T.L. Vincent, Does pain at an earlier stage of chondropathy protect female mice against structural progression after surgically induced osteoarthritis? *Arthritis. Rheum.* 72 (12) (2020) 2083–2093.
- [55] M. Dзамukova, T.M. Brunner, J. Miotla-Zarebska, F. Heinrich, L. Brylka, M.-F. Mashreghi, A. Kusumbe, R. Kühn, T. Schinke, T.L. Vincent, Mechanical forces couple bone matrix mineralization with inhibition of angiogenesis to limit adolescent bone growth, *Nat. Commun.* 13 (1) (2022) 3059.
- [56] J. Hashemi, N. Chandrashekar, B. Gill, B.D. Beynon, J.R. Slauterbeck, R.C. Schutt Jr, H. Mansouri, E. Dabezies, The geometry of the tibial plateau and its influence on the biomechanics of the tibiofemoral joint, *JBJS* 90 (12) (2008) 2724–2734.
- [57] C.R. Safinya, Structures of lipid-DNA complexes: supramolecular assembly and gene delivery, *Curr. Opin. Struct. Biol.* 11 (4) (2001) 440–448.